

A Differential VCO Design for GSM Handset Applications



APN1013

Introduction

The differential pair of bipolar transistors is the common building block in modern RF integrated circuits. An advantage of this architecture is its high loop gain making it popular for differential Voltage Controlled Oscillator (VCO) designs in RFICs. Designers of discrete (or hybrid) VCO circuits usually use the more traditional Colpitts design avoiding the added complexity of the differential VCO configuration.

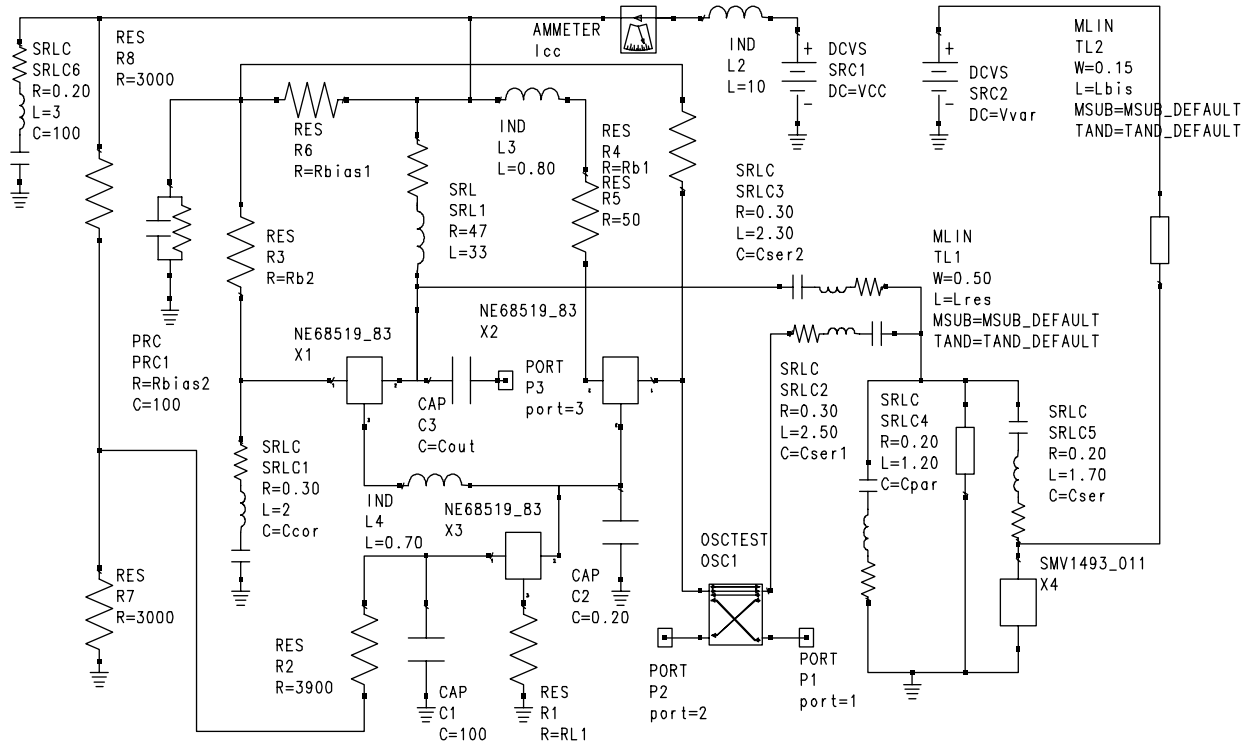
Because of its primary usage in proprietary RFICs, only limited differential VCO design and modeling information has been made available. In this application note, we will attempt to build a bridge toward better understanding of the differential VCO by describing a design covering 910–980 MHz which is appropriate for use in GSM handsets. This design will also demonstrate how the Alpha SMV1493-079 varactor diode, an essential element in this VCO, may be used advantageously in designs aimed at other wireless applications including AMPS, CDMA, and PCS.

The VCO Model

In the circuit in Figure 1 the transistor pair X_1 and X_2 form a differential configuration with X_3 as a current source. All of the transistors are NEC NE68519 with 12 GHz f_T . We chose this transistor for this demonstration because it is commonly used in many VCO applications and its SPICE parameters are available. The RF signal from collector of X_1 is fed through the coupling capacitor SRLC3 to the resonator. The resonator is formed by the parallel connection of capacitive branches SRLC4 and SRLC5/ X_4 ,

and the inductive branch formed by microstrip line TL_1 . The output signal from the resonator is fed through the coupling capacitor SRLC2 to the base of transistor X_2 , which is in differential feedback with X_1 . There it closes the feedback path. Ideally, the phase shift between the base of X_2 and the collector of X_1 in the differential stage is 0° and the oscillation should occur at the exact parallel resonance of the tank circuit. In reality, however, the phase shift in the differential pair is not 0° , because of unavoidable transit times and parasitic reactances.

For example, the phase shift in this loop changes from -50° to -100° in the frequency range of from 0.8–1.5 GHz. To compensate this (capacitive) phase shift, the resonator should be inductive and provide an opposite phase shift. It is interesting to note that compared to the Colpitts VCO configuration, the resonant frequency may be set at the exact oscillation frequency. The Colpitts design can not be used at the natural resonance frequency of the resonator due to losses in the feedback path. Therefore, the differential design has the advantage of both high phase slope at resonance and low loss in the feedback path.



Spice Model for SMV1493-079

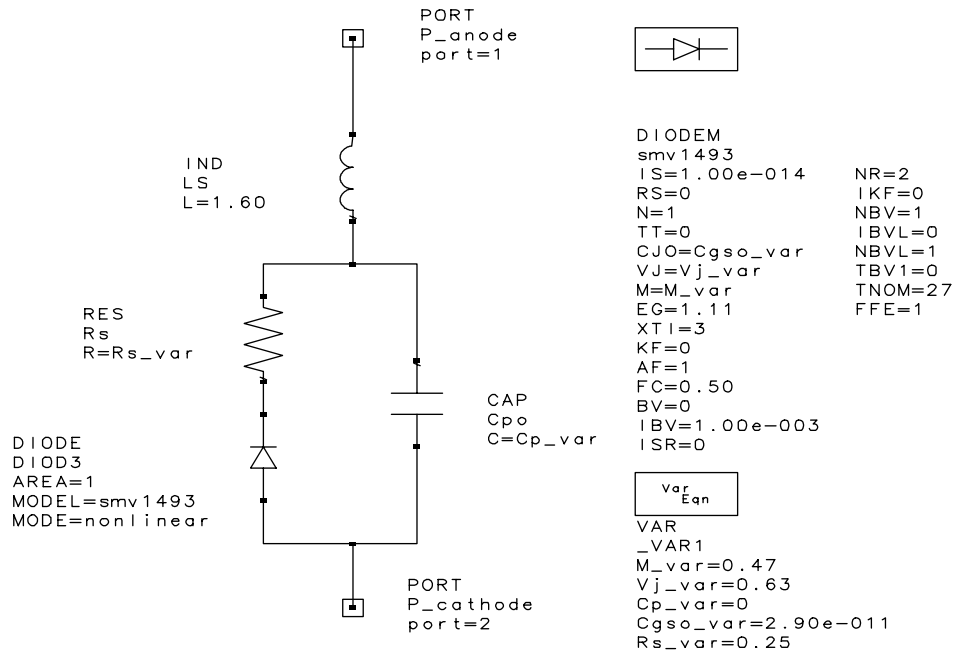


Figure 1. VCO Model Schematic

Capacitors SRLC2 and SRLC3 are used to obtain the required phase shift at the center of the tank circuit resonant frequency. By changing the values of these capacitors, optimum phase noise may be achieved.

Resistor R₅ suppresses higher frequency oscillation modes caused by the parasitic resonance between SRLC4 and varactor branch SRLC5/X₄. A resistance of 20–50 Ω is normally enough to perform this function without serious degradation of loop power and phase noise.

The differential stage bias is set by voltage dividers R₆/PRC1 and R₈/R₇. The base currents are limited by R₃ and R₅ for the differential pair and R₂ for the current source. In this case, the 3 V, V_{CC} current is set to about 7 mA.

In the VCO model test bench in Figure 2 we define open loop gain, $K_u = V_{OUT}/V_{IN}$, as the ratio of voltage phasors at the input and output ports of an OSCTEST component. Defining the oscillation point is a technique to balance input (loop) power to provide zero gain for a zero loop phase shift. Once the oscillation point is defined, the frequency and output power may be “measured.” We do not recommend the use of the OSCTEST2 component for closed loop analysis, since it may not converge and does not allow clear insight to VCO behavior.

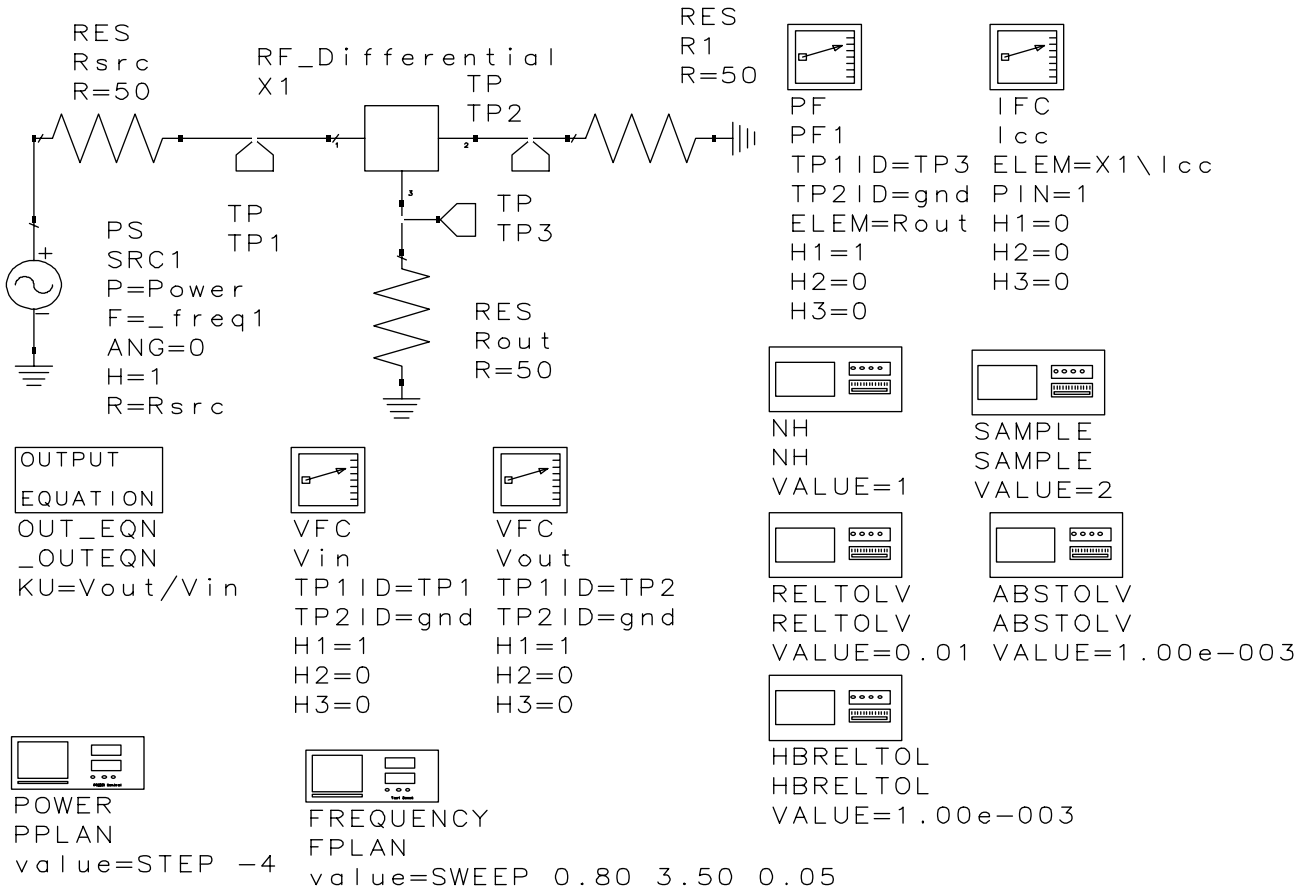


Figure 2. VCO Model Test Bench

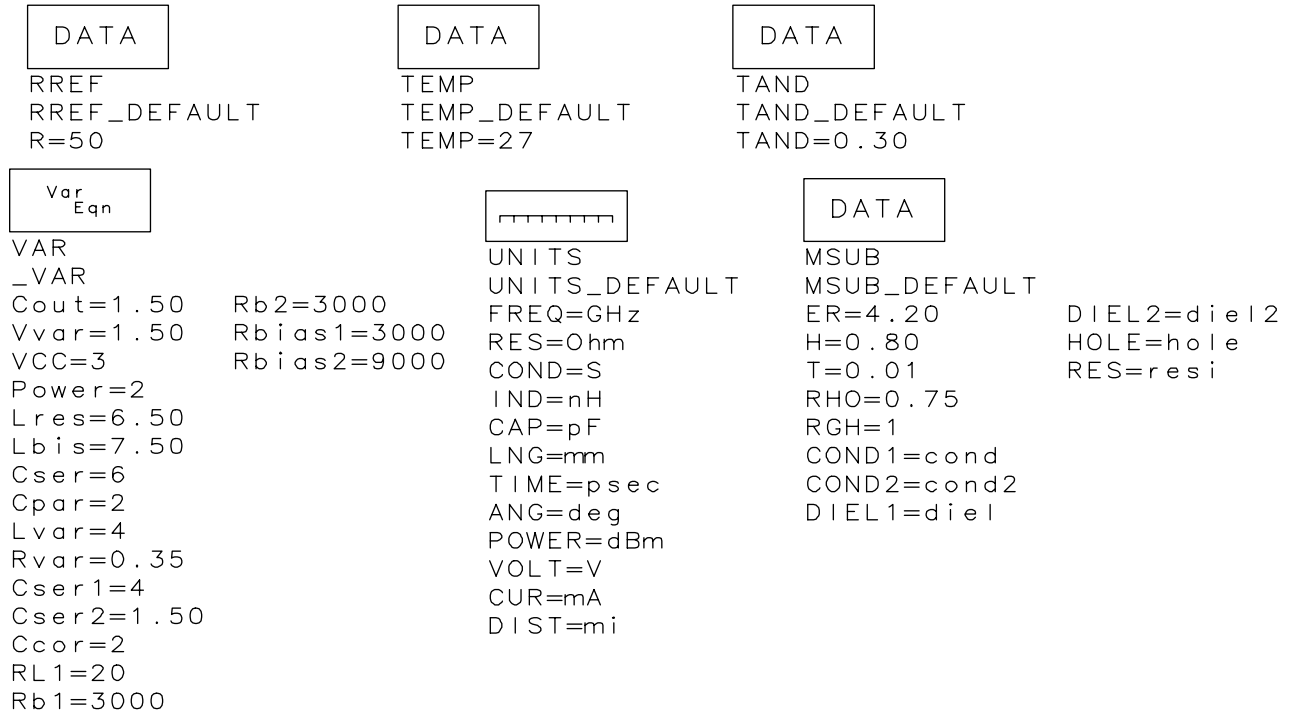


Figure 3. VCO Model Default Bench

Figure 3 shows the default bench where some circuit variables were defined in the “Variables and Equations” component for the convenience of “tuning” during performance analysis and optimization

SMV1493-079 SPICE Model

SMV1493-079 is a low series resistance, hyperabrupt junction varactor diode. It features the industry’s smallest plastic package SC-79 with a body size of 47 x 31 x 24 mm (the total length with leads is 62 mm).

The SPICE model for the SMV1493-079 varactor diode, defined for the Libra IV environment, is shown in Figure 1 with a description of the parameters employed.

Table 1 describes the model parameters. It shows default values appropriate for silicon varactor diodes that may be used by the Libra IV simulator.

Parameter	Description	Unit	Default
IS	Saturation current (with N, determine the DC characteristics of the diode)	A	1e-14
R _S	Series resistance	Ω	0
N	Emission coefficient (with IS, determines the DC characteristics of the diode)	-	1
TT	Transit time	S	0
C _{JO}	Zero-bias junction capacitance (with V _J and M define nonlinear junction capacitance of the diode)	F	0
V _J	Junction potential (with V _J and M define nonlinear junction capacitance of the diode)	V	1
M	Grading coefficient (with V _J and M define nonlinear junction capacitance of the diode)	-	0.5
E _G	Energy gap (with XTI, helps define the dependence of IS on temperature)	eV	1.11
XTI	Saturation current temperature exponent (with E _G , helps define the dependence of IS on temperature)	-	3
KF	Flicker noise coefficient	-	0
AF	Flicker noise exponent	-	1
FC	Forward-bias depletion capacitance coefficient	-	0.5
B _V	Reverse breakdown voltage	V	Infinity
I _{BV}	Current at reverse breakdown voltage	A	1e-3
ISR	Recombination current parameter	A	0
NR	Emission coefficient for ISR	-	2
IKF	High-injection knee current	A	Infinity
NBV	Reverse breakdown ideality factor	-	1
IBVL	Low-level reverse breakdown knee current	A	0
NBVL	Low-level reverse breakdown ideality factor	-	1
T _{NOM}	Nominal ambient temperature at which these model parameters were derived	°C	27
FFE	Flicker noise frequency exponent	-	1

Table 1. Silicon Diode Default Values in Libra IV

According to the SPICE model, the varactor capacitance, C_V, is a function of the applied reverse DC voltage, V_R, and may be expressed as follows:

$$C_V = \frac{C_{JO}}{\left(1 + \frac{V_{VAR}}{V_J}\right)^M} + C_P$$

This equation is a mathematical expression of the capacitance characteristic. The model is accurate for abrupt junction varactors (like Alpha’s SMV1408). For hyperabrupt junction varactors, the model is less accurate because the coefficients are dependent on the applied voltage. To make the equation work better for the hyperabrupt varactors the coefficients were optimized for the best capacitance vs. voltage fit as shown in Table 2 and Figure 4.

Note, that in the Libra model above, C_P is given in picofarads, while C_{GO} is given in farads to comply with the default unit system used in Libra.

Part Number	C _{JO} (pF)	M	V _J (V)	C _P (pF)	R _S (Ω)	L _S (nH)
SMV1493-079	29	0.47	0.63	0	0.25	1.7

Table 2. SPICE Parameters for SMV1493-079

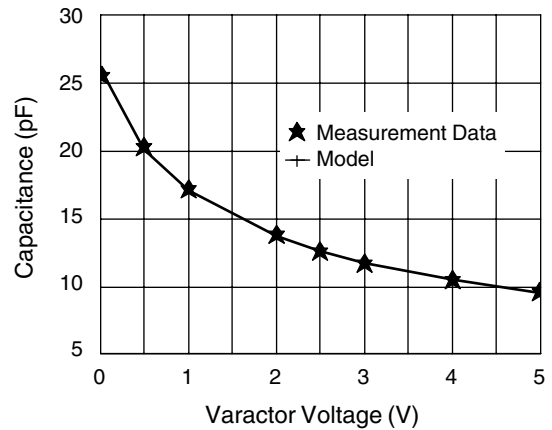


Figure 4. SMV1493-079 C_V Curve

VCO Design, Materials, Layout and Performance

The differential VCO schematic diagram appropriate for a RFIC in many wireless or cordless applications is shown in Figure 5. This circuit is supplied from the 3 V voltage

source. The I_{CC} current is established at approximately 8 mA, and the RF output signal is fed from the VCO through capacitor C_4 (1 pF).

The PCB layout is shown in Figure 6. The board is made of standard 30 mil thick FR4 material.

Table 3 lists the bill of materials.

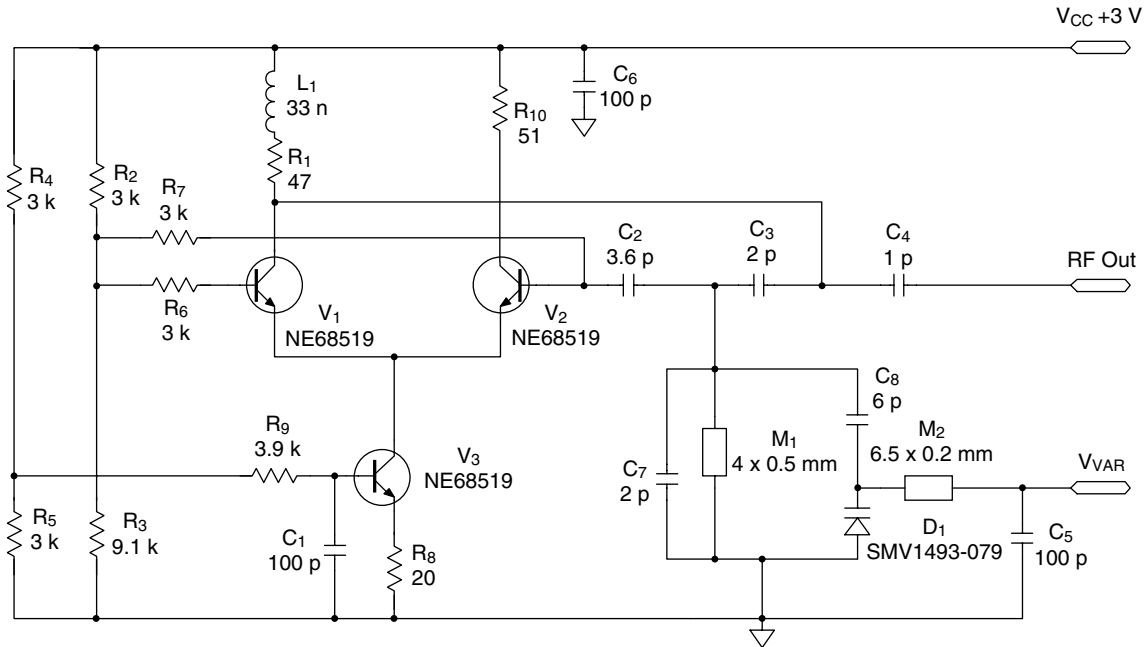


Figure 5. VCO Schematic Diagram

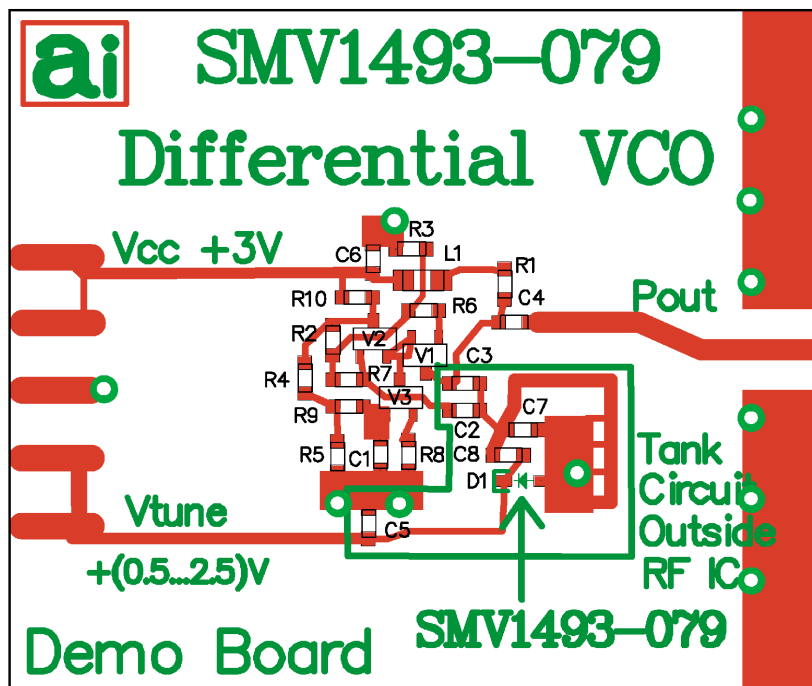


Figure 6. Differential VCO PC Board Layout

Designator	Value	Part Number	Footprint	Manufacturer
C ₁	100 p	0603AU101JAT9	0603	AVX
C ₂	3.6 p	0603AU3R6JAT9	0603	AVX
C ₃	2 p	0603AU2R0JAT9	0603	AVX
C ₄	1 p	0603AU1R0JAT9	0603	AVX
C ₅	100 p	0603AU101JAT9	0603	AVX
C ₆	100 p	0603AU101JAT9	0603	AVX
C ₇	2 p	0603AU2R0JAT9	0603	AVX
C ₈	6 p	0603AU6R0JAT9	0603	AVX
D ₁	SMV1493-079	SMV1493-079	SOD-323	Alpha
L ₁	33 n	0603CS-33NX_BC	0603	Coilcraft
M ₁	4 x 0.5 mm	MSL	4 x 0.5 mm	
M ₂	6.5 x 0.2 mm	MSL	6.5 x 0.2 mm	
R ₁	47	CR10-470J-T	0603	AVX
R ₁₀	51	CR10-510J-T	0603	AVX
R ₂	3 k	CR10-302J-T	0603	AVX
R ₃	9.1 k	CR10-912J-T	0603	AVX
R ₄	3 k	CR10-302J-T	0603	AVX
R ₅	3 k	CR10-302J-T	0603	AVX
R ₆	3 k	CR10-302J-T	0603	AVX
R ₇	3 k	CR10-302J-T	0603	AVX
R ₈	20	CR10-200J-T	0603	AVX
R ₉	3.9 k	CR10-392J-T	0603	AVX
V ₁	NE68519	NE68519	SOT-416	NEC
V ₂	NE68519	NE68519	SOT-416	NEC
V ₃	NE68519	NE68519	SOT-416	NEC

Table 3. VCOs Bill of Materials

The measured performance of this circuit and the simulated results obtained with the model are shown in Figure 7.

Fairly good compliance of frequency response vs. varactor tuning voltage confirms the validity of the varactor model for predicting the frequency behavior of the VCO. However, the power response simulation indicates more variation of power in the tuning range than the measured response. This may be due to the transistor modeling accuracy or the accuracy of the overall VCO model. For example, simulations show that the power may strongly depend on high order harmonics which may not be accurately described by the VCO model.

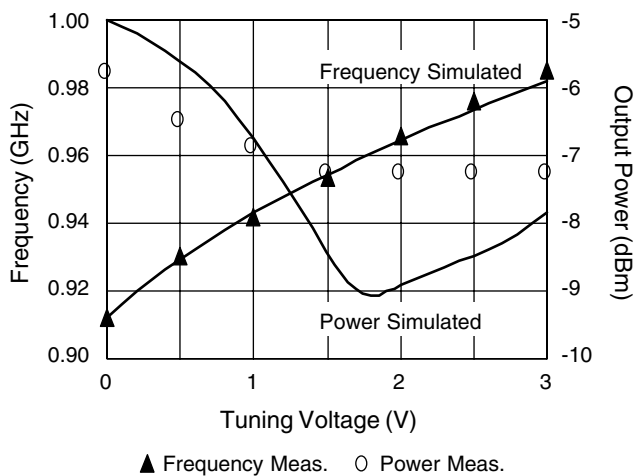


Figure 7. Measured and Simulated Frequency and Power Responses of the Differential VCO

Figure 8 shows the phase noise of the VCO measured in the range of 100 Hz to 8 MHz offset from the carrier. This measurement was made using the Aeroflex PN9000 Phase Noise Test Set with a 40 ns delay line. The best phase noise occurred with circuit components very close to the originally established values in the preliminary simulation. Only small changes were introduced such as: C_2 from its original 4 pF to 3.6 pF, C_3 from 1.5 pF to 2 pF and C_4 from 1.5 pF to 1 pF.

Phase noise was approximately -93 dBc/Hz at a 10 kHz offset, which is about 5–10 dB poorer than a typical Colpitts low noise VCO having similar bias condition. The reason for the poorer phase noise may be that the resonator in a differential VCO works at its resonance frequency (or very near to it). This results in high reactive currents in the resonator, causing high power losses causing much higher phase noise sensitivity to resonator

component losses. This was confirmed by replacing the resonator circuit components with similar ones having less loss. For example, after exchanging the varactor with a lower loss discrete ceramic capacitor, the phase noise was improved by 5–6 dB. In another example, increasing the solder thickness on the microstrip line improved phase noise as much as 3 dB. In comparison, typically there is less phase noise sensitivity to circuit components in a Colpitts VCO design, where the oscillation frequency is always below the resonance frequency of the resonator.

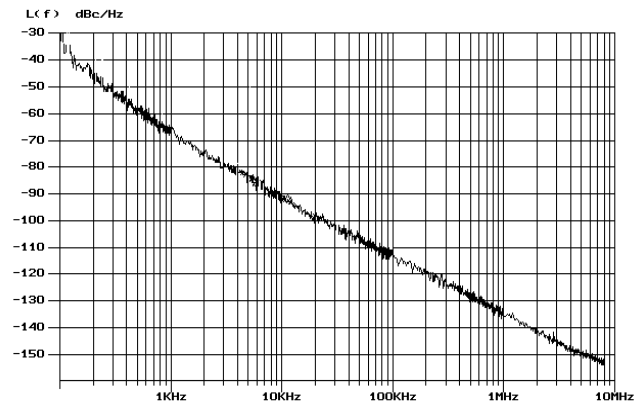


Figure 8. The VCO Phase Noise vs. Carrier Offset Frequency

List of Available Documents

The Differential RF VCO Simulation Project Files for Libra IV.

The Differential RF VCO Circuit Schematic and PCB Layout for Protel EDA Client, 1998 Version.

The Differential RF VCO PCB Gerber Photo-plot Files.

VCO Related Application Notes

APN1004, "Varactor SPICE Models for RF VCO Applications."

APN1006, "A Colpitts VCO for Wideband (0.95– 2.15 GHz) Set-Top TV Tuner Applications."

APN1005, "A Balanced Wideband VCO for Set-Top TV Tuner Applications."

APN1007, "Switchable Dual-Band 170/420 MHz VCO for Handset Cellular Applications."

"An RF VCO Design for Wireless and Broadband Applications."